Semiconductor Optoelectronics, *Vol. 42 No. 2 (2023), 438-446*
https://bdtgd.cn/

Semiconductor Optoelectronics
ISSN: 1001-5868

A SILICON-ON-INSULATOR RING RESONATOR ASSISTED MACH ZEHNDER INTERFEROMETER STRUCTURE FOR HIGHLY SENSITIVE HYDROGEN INTENSITY DETECTION

Trung Thanh Le[*,a], Duy Tien Le[a], The Duong Do[b], Thi Hong Loan Nguyen[c] and Anh Tuan Nguyen[a]

[a*]International School (VNU-IS), Vietnam National University (VNU), Hanoi, 1000000, Vietnam.

[b]University of Transport and Communications (UTC), Hanoi, 1000000, Vietnam

[c]University of Natural Resources and Environment, Hanoi, 1000000, Vietnam

Abstract:

We propose a new highly sensitive hydrogen sensor based on a ring resonator (RR) assisted Mach Zehnder Interferometer (MZI) in silicon waveguides. Based on the Fano like effect generated from the resonator structure, the sensor's sensitivity is achieved with 10 orders higher than the typical sensor based on single microring resonator and Mach Zehnder Interferometer (MZI). The device is highly sensitive to low hydrogen concentration variations of from 0-4% in the range of hydrogen's lower flammability limit (EFL). We also optimally design the gap and width of the palladium (Pd) covered in the sensing area for low loss, but still achieve the low detection limit and high sensitivity. This optical hydrogen sensor can provide capabilities for ease of fabrication, ease of fabrication, low fabrication tolerance compared with optical sensors based on only directional couplers.

Keywords: Multimode interference (MMI), ring resonator, integrated optics, optical sensor, hydrogen sensor, silicon photonics.

1. Introduction

Hydrogen has been widely employed as a fuel source in a variety of applications, including chemical industrial production, oil and gas refineries, aerospace, and automobile industries [1, 2]. If the calorific value of hydrogen is high enough, it will become a competitive energy transporter. However, the public use and storage of the hydrogen is also dangerous. A higher hydrogen level higher than lower flammability limit (4%) of hydrogen can cause a serious explosion. As a result, developing a fast and reliable gas sensor for hydrogen detection is critical for its safe storage, handling, and use.

Numerous hydrogen sensors are readily accessible in today's market. Many of these sensors are grounded in principles of hydrogen detection that have been established for several decades [3]. Nevertheless, in the pursuit of aligning with the demands of an emerging hydrogen-centric economy, significant ongoing research endeavors are focused on the continuous enhancement of sensor performance. This improvement encompasses facets such as selectivity, sensitivity, and response time, alongside the goals of reducing sensor dimensions, cost, and power consumption.

Various types of hydrogen sensors have been developed including catalytic, electrochemical, metal-oxide semiconductor, and optical hydrogen sensors [4]. Among those, the latter provides a number of advantages owing to their compact size, safety, and immunity from electromagnetic interference. Particularly, optical fiber-based hydrogen sensors are amongst emerging devices. They have good sensitivity and multiplexing capabilities. Unfortunately, they are less suitable for integration due to their bulk, thus limiting their potentials in densely integrated on-chip applications. The capability of integrating the sensor provides more advantages such as high compactness and cheap large-scale-integration fabrication.

In addition, recent hydrogen sensors based on single ring resonator on silicon on insulator (SOI) technology with Pd/Pt cover [4], ZnO cover [5] or MZI structure with WO3/Pt covering [6]. These structures are limited in sensitivity. The aim of this research is to find out a new structure in order to provide a high sensitivity. In this paper, we present an MZI with a ring resonator structure to generate the Fano effect applied for hydrogen detection. Two multimode interference couplers (MMI) are used. We showed that MMI based sensors have advantages of compactness, large fabrication tolerance, small insensitivity to temperature fluctuation and ease of fabrication [7, 8]. Our structure can generate the Fano line shape. As a result, it can provide an ultra-high sensitivity compared with the conventional structures. 3D EME (EigenMode Expansion) and FDTD (Finite Difference Time Difference) simulations are used for the whole design of the sensor.

2. Proposal of the new high sensitive hydrogen sensor

The proposed structure based on two MMI couplers integrated with a single ring resonator is presented in Fig.1(a). In this design, we use an SOI waveguide with the following parameters: the height of 220nm and the width of 500nm. At operating wavelength around 1550nm, the waveguide is single mode waveguide. The structure parameters of the ring resonator integrated with one arm of the MZI are shown in Fig.1(b).

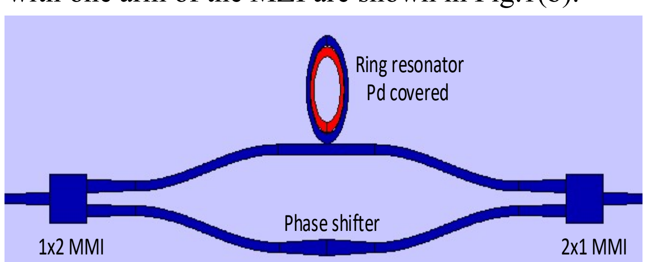

(a)

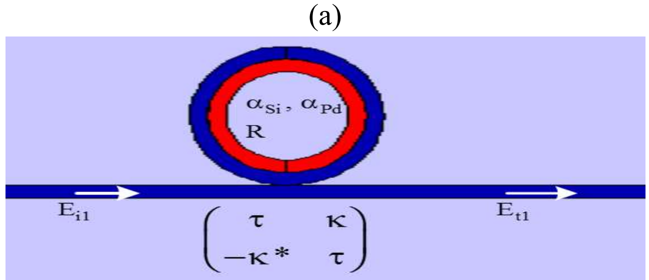

(b)

Fig 1. Hydrogen sensor structure

In order to generate the Fano effect, at another output port of Fig.1(a), we use a phase shift based on wider waveguide to create a phase shift of 0.5 π (rad).

In this research, we use a ring resonator fully covered with the Pd layer as shown in Fig.1(b). The complex refrective index of the Pd at 1550nm is n=3.605 + 8.498i [9]. The variations of the real and imaginary parts of the Pd RI with wavelength are given in Fig. 2. The real and imaginary parts of the Pd refractive index vary with the thickness of the layer. With the presence of hydrogen, the refractive index of the Pd layer changes, leading to changes in the resonance characteristics of the ring resonator and therefore chainging in the normalized output power of Fig.1(a). The experimentally reports showed that both real and imaginary parts of the permittivity of the Pd films decrease with the adsorption of hydrogen [9]. The real and imaginary parts of the RI (n and k) as a function of the real and imaginary parts of the permittivity (ε1 and ε2) are given as:

$$n = \sqrt{\frac{\sqrt{\varepsilon_1^2 + \varepsilon_2^2} + \varepsilon_1}{2}}, \qquad k = \sqrt{\frac{\sqrt{\varepsilon_1^2 + \varepsilon_2^2} - \varepsilon_1}{2}} \qquad (1)$$

Thus when ε1 and ε2 decrease, the real part n will also decrease and the imaginary part k may increase or decrease depending on the value of the permittivity. Thus the real part of the Pd refractive index decreases on hydrogen adsorption.

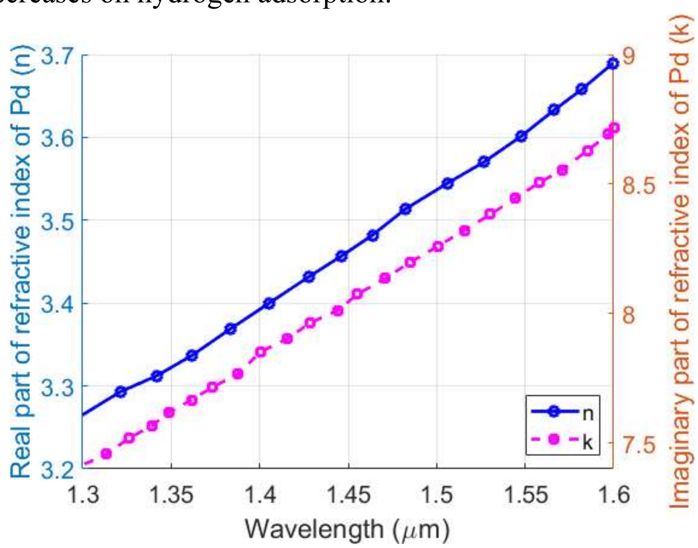

Fig 2. Real and imaginary parts of Pd

Due to the presence of the Pd layer around the SOI waveguide, the loss factor will be significantly increase. Therefore, we need to optimally design the gap between the Pd layer and the SOI waveguide to reduce the loss, but still keep the hydrogen absorption large enough. By using the 3D EME simulation, we calculate the complex effective index of the TE like mode at different gaps for 0%H2 and 2%H2 for example. The real part of the effective index and the loss factor are shown in Fig.3(a) and (b), respectively. Therefore, we can choose a gap of 10nm for loss reduction.

At the optimal gap of 10nm, the mode profile of the waveguide in the ring resonator is shown in Fig.4(a) and Fig.4(b) shows the field propagation via the ring resonator at the operating wavelength of 1550nm. The ring radius is 5μm . In Fig.1(a), the sensing area is within the ring resonator.

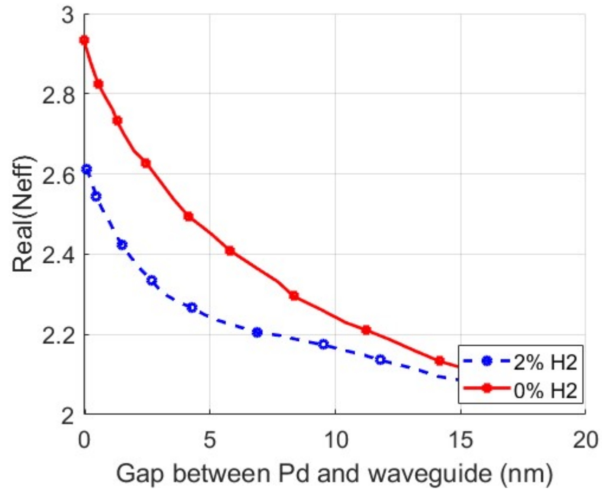

(a)

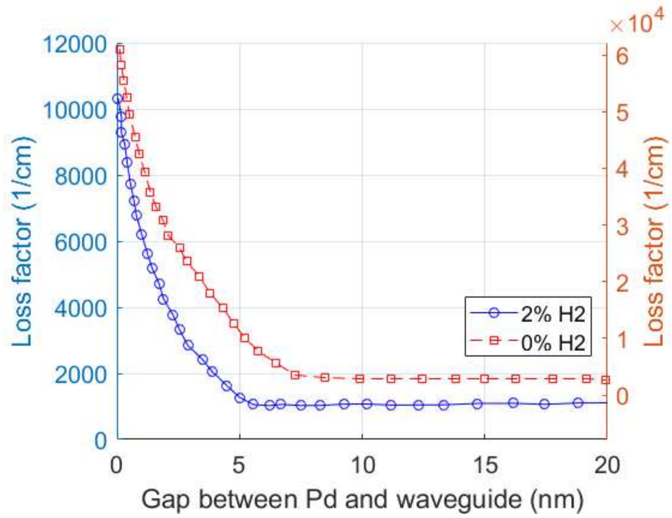

(b)

Fig 3. (a) Real effective refractive index and (b) loss factor at different gaps between the Pd layer and the SOI waveguide

For a single ring resonator, we use this region for sensing region in Fig.1(a). The coupling element for ring resonator is a directional coupler, where κ and τ are the cross-coupling coefficient and transmission-coupling coefficient of the microring resonator coupler; α is the attenuation factor of the field after one round trip through the ring waveguide. The complex electric fields at output of the ring resonator in the sensing area of Fig.1(b) is expressed by using the Yariv's model [10]:

$$\begin{pmatrix} E_{t1} \\ E_{t2} \end{pmatrix} = \begin{pmatrix} \tau & \kappa \\ -\kappa^* & \tau \end{pmatrix} \begin{pmatrix} E_{i1} \\ E_{i2} \end{pmatrix} \qquad (2)$$

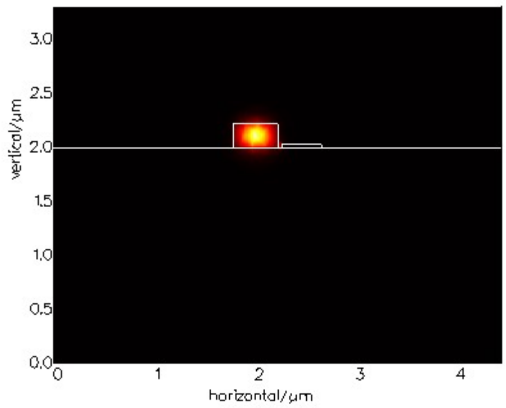

(a)

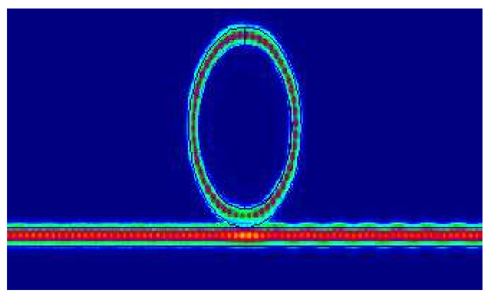

(b)

Fig 4. (a) Field profile and (b) field propagation through the sensing area

where $E_{i2} = \alpha \exp(j\phi) E_{t2}$, n_{eff} is the effective index and L_R is the microring resonator length. The loss factor of the Pd covered microring resonator can be expressed by

$$\alpha = \exp(-0.5\alpha_{Pd} L_{Pd}) \exp[-0.5\alpha_{Si}(2\pi R - L_{Pd})] \quad (3)$$

where R is the radius of the microring and $\alpha_{Si}[dB/cm]$ is the loss coefficient of the Si waveguide. The output field and input field of a single microring resonator is:

$$E_{t1} = E_{i1} \frac{-\alpha + \tau e^{-j\phi}}{-\alpha\tau^{*} + e^{-j\phi}} \quad (4)$$

The round trip phase ϕ of the ring resonator is calculated by:

$$\phi = \frac{2\pi}{\lambda}[n_{eff}^{Pd} L_{Pd} + n_{eff}^{Si}(2\pi R - L_{Pd})] \quad (5)$$

For sake of simplicity, we choose the gap of the directional coupler 90nm to design a 3dB coupler [7]. The normalized transmitted power at the output waveguide of the single ring resonator is expressed by [10]:

$$T = \left|\frac{E_{t1}}{E_{i1}}\right|^2 = \frac{\alpha^2 - 2\alpha\tau\cos(\phi) + \tau^2}{1 - 2\alpha\tau\cos(\phi) + \alpha^2\tau^2} \quad (6)$$

From equation (4), the phase of the single ring resonator is

$$\phi_{single} = \Delta\varphi = \text{artan}\left\{ \frac{\alpha\kappa^2 \sin(\omega)}{\left(1+\alpha^2\right)\tau - \left(1+\tau^2\right)\alpha\cos(\omega)} \right\} \tag{7}$$

where ω is the angular frequency.

Based on matrix calculation approach, we can find out the intensity of the sensing structure is

$$I = \left| \cos\left(\frac{1}{2}\text{artan}\left\{ \frac{\alpha\kappa^2 \sin(\omega)}{\left(1+\alpha^2\right)\tau - \left(1+\tau^2\right)\alpha\cos(\omega)} \right\}\right) \right|^2 \tag{8}$$

3. Simulation Results and Discussions

In this study, we use the intensity mechanism for hydrogen detection. With the presence of H2, the effective index n_{eff} will be changed due to the presence of the Pd layer around the SOI waveguide. This results in a change in the output intensity.

The complex permittivity of the Pd after hydrogen absorption can be expressed by [11]:

$$\varepsilon(Pd,\%H_2) = h(\%H_2)x\varepsilon(Pd,0\%H_2) \tag{9}$$

where $\varepsilon(Pd,0\%H_2)$ is the complex permittivity of the pure Pd layer and $h(\%H_2)$ is the function depending on hydrogen concentration.

The sensitivity of the hydrogen sensor of Fig.1(a) is expressed by [12, 13]

$$S = \frac{\partial I}{\partial n_a} = \frac{\partial I}{\partial \lambda}\frac{\partial \lambda}{\partial n_{eff}}\frac{\partial n_{eff}}{\partial n_a} = S_1S_3S_3\,(nm/\,RIU) \tag{10}$$

where ∂I is the intensity change of the optical signal and $\partial\lambda$ is the wavelength shift; $S_2 = \frac{\partial\lambda}{\partial n_{eff}} \approx \frac{\lambda}{n_{eff}}$ is the resonant wavelength range which enabled by the resonance lineshape. In the intensity mechanism, it is almost a constant and is determined by the working wavelength. In our design, we choose the working wavelength of 1550nm for compatibility with fiber-optic communication systems. Therefore, the sensor can be connected to current optical communication systems for long distance monitoring applications. $S_3 = \frac{\partial n_{eff}}{\partial n_a}$ is defined as the shift in effective refractive index caused by the change in sensing region and can be optimized by waveguide cross-section design.

Therefore, the aim of most important studies is to find the way to increase $S_1 = \frac{\partial I}{\partial \lambda}$. Our proposed structure can create the Fano lineshape, therefore factor S_1 can be increased compared much with the MZI configuration or single microring resonator. In literature, the Mach Zehnder interferometer and ring resonator can be used, but the slopes of these structures are low. The responses of the sensor structure at 0%H2 and 1%H2 for example are shown in Fig.4

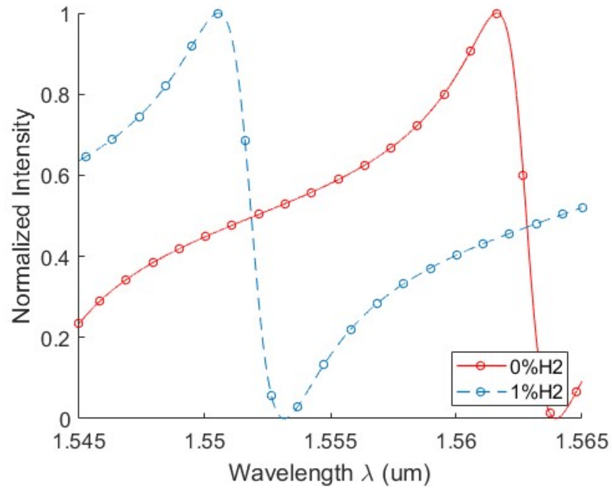

Fig. 5. The slope of the transmission

We compare the proposed structure with conventional structures based on MZI and microring resonators as shown in Fig.6. It is shown that the slope of the proposed structure is higher than 10 times compared with the conventional structure. As a result, this sensor can provide a higher sensitivity of 10 times compared with sensor structures based on the conventional MZI and microring resonator.

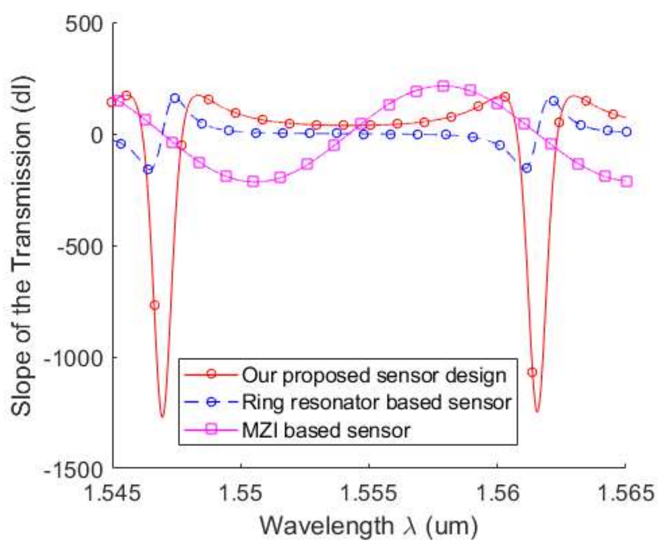

Fig. 6. The slope of the transmission

Finally, we use the FDTD to simulate the responses of the sensor for different %H2. The simulations are shown in Fig.7 for 0%H2, 1%H2, 2%H2 and 3%H2 respectively. The FDTD simulations also show that a high sensitivity can be achieved.

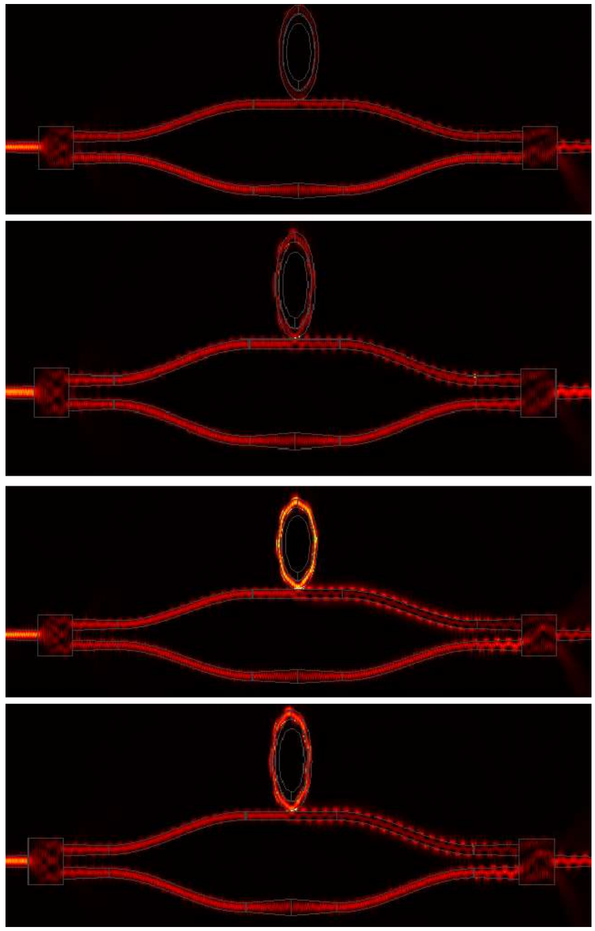

Fig. 7. FDTD simulations for the working principle of the sensor

For the intensity based sensor, the LOD (Limit of Detection) represents the minimal detectable amount of %H2. In intensity-based detection, LOD can be expressed as:

$$\mathrm{LOD} = \frac{\delta I}{S} \tag{11}$$

where δI is the intensity uncertainty of the sensor limited by the systems noises, which consist of thermal noise, intensity noise and spectral noise [13]:

$$\mathrm{LOD} = \sqrt{\mathrm{LOD}^2_{\mathrm{Thermal}} + \mathrm{LOD}^2_{\mathrm{Spectral}} + \mathrm{LOD}^2_{\mathrm{Intensity}}} \tag{12}$$

4. Conclusions

We have presented a new hydrogen sensor structure based on intensity mechanism for ultra-high sensitivity using the MZI integrated with a microring resonator. The sensor can provide a higher sensitivity order of 10 times compared with the MZI and ring resonator conventional structures. The sensor was designed using silicon waveguide that is cheap and compatible with the current existing CMOS technology. The proposed sensor structure can be integrated with fiber-optic communications for real time and online applications in the future.

Acknowledgement

This research is funded by Vietnam National University, Hanoi (VNU) under pro-ject number QG.19.58

References

[1] Y. S. Yi, D. C. Wu, P. Birar, and Z. Yang, "Ring Resonator-Based Optical Hydrogen Sensor," *IEEE Sensors Journal,* vol. 17, no. 7, pp. 2042-2047, 2017, doi: 10.1109/JSEN.2017.2669521.

[2] S. Garg, V. Mishra, L. F. Vega, R. S. Sharma, and L. F. Dumée, "Hydrogen Biosensing: Prospects, Parallels, and Challenges," *Industrial & Engineering Chemistry Research,* vol. 62, no. 11, pp. 4676-4693, 2023/03/22 2023, doi: 10.1021/acs.iecr.2c03965.

[3] A. K. Pathak, S. Verma, N. Sakda, C. Viphavakit, R. Chitaree, and B. M. A. Rahman, "Recent Advances in Optical Hydrogen Sensor including Use of Metal and Metal Alloys: A Review," *Photonics*, vol. 10, no. 2*,* doi: 10.3390/photonics10020122.

[4] G. Mi, C. Horvath, and V. Van, "Silicon photonic dual-gas sensor for H2 and CO2 detection," *Optics Express,* vol. 25, no. 14, pp. 16250-16259, 2017, doi: 10.1364/OE.25.016250.

[5] N. A. Yebo, P. Lommens, Z. Hens, and R. Baets, "An integrated optic ethanol vapor sensor based on a silicon-on-insulator microring resonator coated with a porous ZnO film," *Optics Express,* vol. 18, no. 11, pp. 11859-11866, 2010, doi: 10.1364/OE.18.011859.

[6] S. Matsuura, N. Yamasaku, Y. Nishijima, S. Okazaki, and T. Arakawa, "Characteristics of Highly Sensitive Hydrogen Sensor Based on Pt-WO3/Si Microring Resonator," *Sensors,* vol. 20, no. 1, 2020, doi: 10.3390/s20010096.

[7] D.-T. Le, M.-C. Nguyen, and T.-T. Le, "Fast and slow light enhancement using cascaded microring resonators with the Sagnac reflector," *Optik - International Journal for Light and Electron Optics,* vol. 131, pp. 292–301, Feb. 2017.

[8] J. Capmany, D. Domenech, and P. Muñoz, "Silicon graphene Bragg gratings," *Optics Express,* vol. 22, no. 5, pp. 5283-5290, 2014, doi: 10.1364/OE.22.005283.

[9] L. Goddard, W. Kai Yeen, A. Garg, E. Behymer, G. Cole, and T. Bond, "Measurements of the complex refractive index of Pd and Pt films in air and upon adsorption of H<inf>2</inf> gas," in *LEOS 2008 - 21st Annual Meeting of the IEEE Lasers and Electro-Optics Society*, 9-13 Nov. 2008 2008, pp. 569-570, doi: 10.1109/LEOS.2008.4688745.

[10] A. Yariv, "Universal relations for coupling of optical power between microresonators and dielectric waveguides," *Electronics Letters,* vol. 36, pp. 321–322, 2000.

[11] K. Q. Le and Q. M. Ngo, "A silicon-on-insulator surface plasmon interferometer for hydrogen detection," *Journal of Applied Physics,* vol. 120, no. 4, p. 043106, 2016, doi: 10.1063/1.4959261.

[12] T.-T. Le, "Realization of a Multichannel Chemical and Biological Sensor Using 6x6 Multimode Interference Structures," *International Journal of Information and Electronics Engineering, Singapore,* vol. 2, pp. 240-244, 2011.

[13] X. Zhou *et al.*, "On-Chip Biological and Chemical Sensing With Reversed Fano Lineshape Enabled by Embedded Microring Resonators," *IEEE Journal of Selected Topics in Quantum Electronics,* vol. 20, no. 3, pp. 35-44, 2014, doi: 10.1109/JSTQE.2013.2294465.